Structural Analysis of "T" and "KT" Joints of a Steel Truss Structure Using the Finite Element Method

L.F. Costa Neves[1], Luciano R. O. de Lima[2], S. Jordão[3], J. G. S. da Silva[4]

[1]Assistant Professor, Civil Engineering Department,
University of Coimbra, Portugal. Structural Engineer, Struplano Ltd – luis@dec.uc.pt
[2]Associate Professor, Structural Engineering Department,
UERJ - State University of Rio de Janeiro, Brazil - luciano@dec.uc.pt
[3]Assistant, Civil Engineering Department,
University of Coimbra, Portugal – sjordao@dec.uc.pt
[4]Associate Professor, Mechanical Engineering Department,
UERJ - State University of Rio de Janeiro, Brazil - jgss@eng.uerj.br

Abstract

The structural analysis of an outdoor footbridge designed as a 3D tubular steel truss structure is presented. Special emphasis was given to the study of the joints, of two different types: a "T"-joint and a "KT"-joint. Their behaviour is discussed and analysed using the Eurocode 3 methods and finite element models. These numerical models are extensively presented and discussed, reflecting the performed linear and both full material and geometric non linear analysis. An assessment of the applicability and accuracy of the code models is discussed, by comparing their results to the numerical results.

Keywords: Steel structures, structural engineering, finite element analysis, semi-rigid behaviour, plastic analysis, non-linear analysis, second order analysis, joints.

1 Introduction

The analysed structural system represents an outdoor footbridge spanning 27 meters between different parts of a building (Figure 1) with a total construction area of 81,000 square meters, divided in 25 sub-structures. Although maximum number of storeys is 12 (with a maximum of 5 storeys above ground level), in this particular zone the number of storeys is only of 3, that makes any solution for the steel structure easier to erect.

The system is supported at both ends by the major reinforced concrete structures using adequately designed corbels. For the design of the structural elements, a linear global elastic analysis was performed, and the elements checked according to the Eurocode 3, EN 1993-1-1 [1]. Chords are made of 300×8 RHS sections and the braces of 260×8 RHS sections.

Emphasis is given to the outdoor footbridge joints. Two types of joints were studied, identified and detailed in Figure 2: a “T” joint and a “KT” joint, both unreinforced, except the end nodes, near the supports.

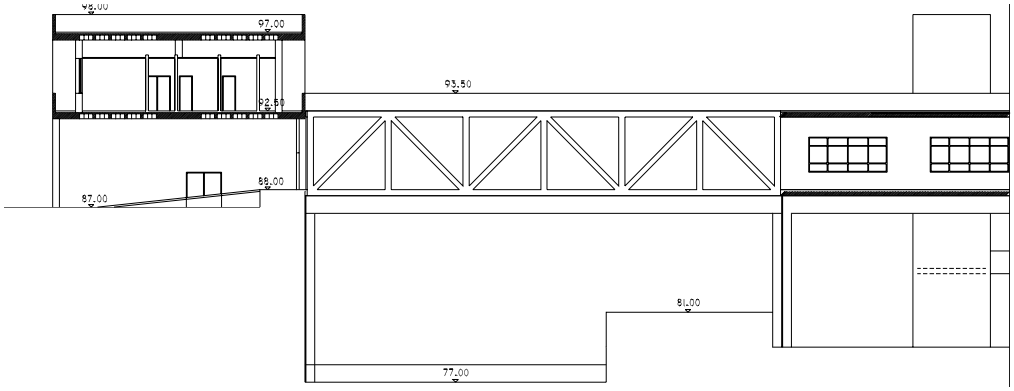

Figure 1: Outdoor footbridge.

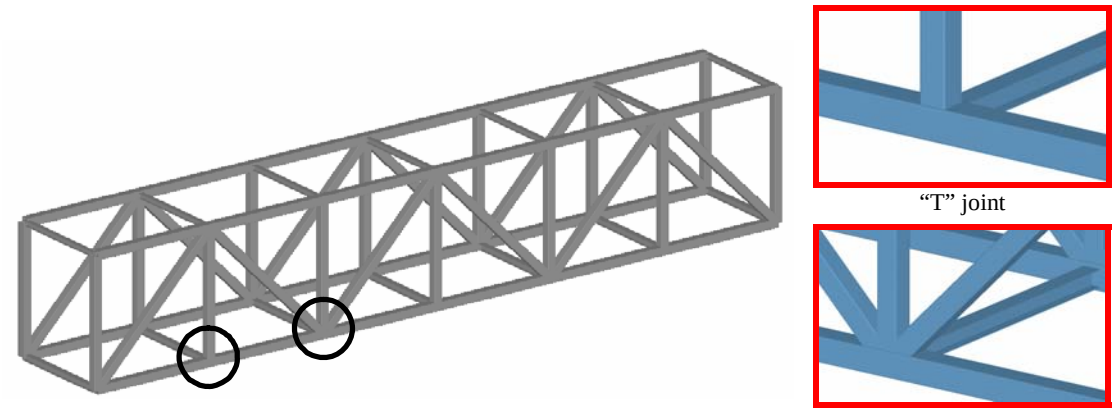

Figure 2: Model of the footbridge and analysed joints.

2 Analysis and Design of Hollow Section Joints

Traditionally, design rules for hollow sections joints are based either on plastic analysis either on deformation limits criteria.

The use of plastic analysis to define the joint ultimate limit sate is based on a plastic mechanism corresponding to the assumed yield line pattern. As examples, the studies of *Cao et al* [2], *Packer* [3], *Packer et al* [4] and *Kosteski et al* [5] may be referred. Each plastic mechanism is associated to an ultimate load, more accurate for more adequate mechanisms. These authors adopted for the yield lines, straight, circular, or a combination of both patterns. *Packer et al* [4] have assumed these three patterns, concluding that the best approximation (if compared to experimental results) was the straight lines mechanism, with an optimising parameter.

However, some of these authors found that for large values of the parameter β (β is the brace width to chord width - see Figure 3), these mechanisms could give a very poor and unsafe prediction of the ultimate load. In fact, the solutions from these bending mechanisms tend to infinity when the parameter β tends to 1 (Figure 4). *Packer et al* [4] found that when $\beta \geq 0{,}95$ the theoretical bending load could be of only 12% of the corresponding experimental load. These authors have then proposed pure shear mechanisms, and concluded that their application to these cases overestimate the experimental load as well, with the theoretical load of only 30% of the corresponding experimental load.

Davies and Packer [6] have proposed plastic mechanisms taking into account bending and punching shear, and found that the corresponding results are a considerable improvement of accuracy, since they overestimate the experimental load of about 20%.

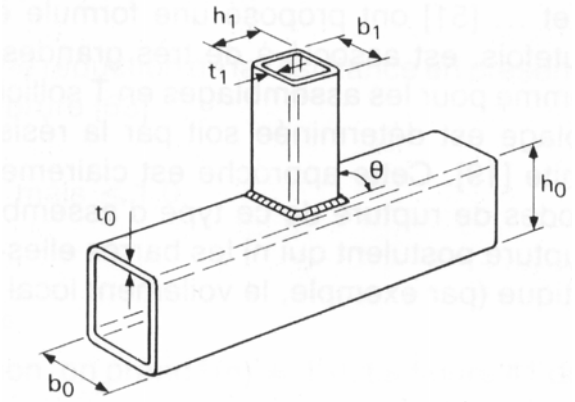

$$\beta = \frac{b_1}{b_0} \qquad \mu_1 = \frac{b_1}{t_1}$$

$$\mu_0 = \frac{b_0}{t_0} \qquad \gamma = \frac{b_0}{2t_0}$$

Figure 3: Geometry and governing parameters.

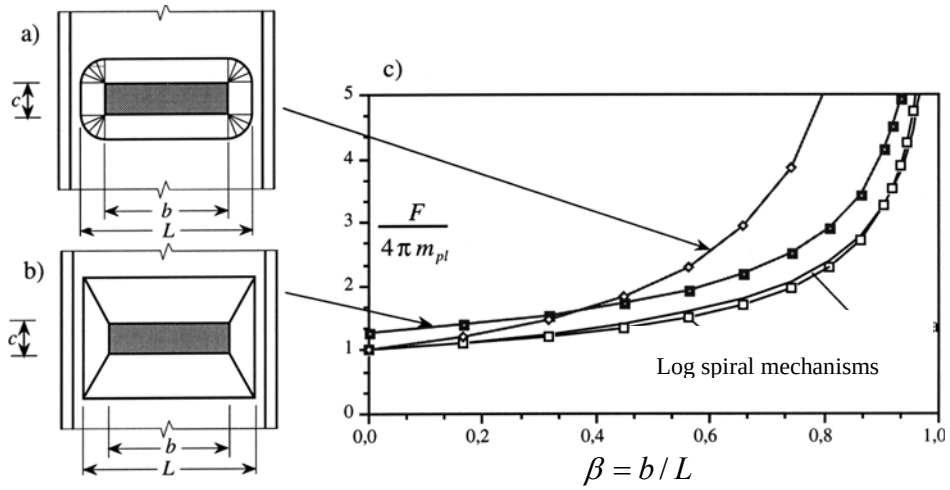

Figure 4: Log spiral mechanisms and other patterns mechanisms.

Gomes [7], in the context of minor axis joints, developed plastic mechanisms with yield log-spiral fans that considerably reduce the plastic load for bending, as shown in Figure 4. This author developed as well mechanisms taking into account bending and punching shear simultaneously, all directly applicable to RHS joints [4] but not, until the present, adopted on any code provisions.

Deformation limits criteria usually associate the ultimate limit state of the chord face to a maximum out of plane deformation of this component. *Korol and Mirza* [8] proposed that the ultimate limit state should be associated to a chord face displacement of 1.2 times its thickness, as this value corresponded to about 25 times the chord face elastic deformation. *Lu et al* [9] proposed that the joint ultimate limit state should be associated to an out of plane deformation equal to 3% of the face width, corresponding to the maximum load reached in their experimental study. This 3% limit was proposed as well by *Zhao* [10], and is actually adopted by the *International Institute of Welding* to define the ultimate limit state.

Kosteski *et al* [5] have compared results from the plastic analysis to the above referred deformation limit (3%), and concluded that if punching shear is not the ruling mechanism, results are within a 20 % approximation range.

The justification for a deformation limit criterion instead of the use of plastic analysis for the prediction of the ultimate limit state is that, for slender chord faces, the joint stiffness does not vanish after complete yielding, but may assume quite large values due to membrane effects. This phenomenon is clearly shown in the curves obtained from the material and geometrical nonlinear analysis in the context of the present study. It is evident that, if the maximum load is obtained from experimental curves, the absence of a “knee” in the curve could make difficult to identify this ultimate limit state point. Besides, comparison of experimental and plastic analysis results need, in these cases, to be based on a deformation criterion as well.

The full exploitation of this additional membrane resistance is not compatible with the allowed displacements within the joint. Besides, if the chord is subjected to cyclic loading, or the chord is subjected to compressive axial loading, membrane overstrength no longer will be significant [11]. As a consequence, the most effective and correct way to define these joints ultimate limit state, besides adequate numerical or experimental testing, is the analytical way using plastic analysis, incorporating punching shear and instability phenomena.

3 Eurocode 3 Provisions

The Eurocode 3 part 1-8 (EN 1993-1-8) [12] proposes for the prevision of the rotational behaviour of beam-to-column, beam-to-beam or column base joints, a general methodology, known as the “component method”. It is based on a mechanical model composed of rigid links and extensional springs where each spring representing a source of deformability known as the component. Each of

these components is then characterised separately in terms of translational behaviour, and their assemblage results in the moment-rotation curve of the whole joint. However, for connections between RHS joints, such as the represented in Figure 2, a different approach is usually adopted. It is based on the assumption that these joints are pinned and therefore the relevant characteristic (besides to the deformation capacity) is the resistance of the chord and braces, all subjected primarily to axial forces.

These Eurocode 3 [12] provisions for the evaluation of design joint resistance of connections between hollow sections assume the following failure modes:

- plastic failure of the chord face Figure 5(a);
- chord side wall failure by yielding, crushing or instability under the compression brace member Figure 5(b);
- chord plastification (plastic failure of the chord cross section);
- chord shear failure Figure 5(c);
- punching shear failure of a hollow section chord wall Figure 5(d);
- brace failure with reduced effective width Figure 5(e);
- local buckling failure of a brace member, or of an hollow section chord member at the joint location Figure 5(f).

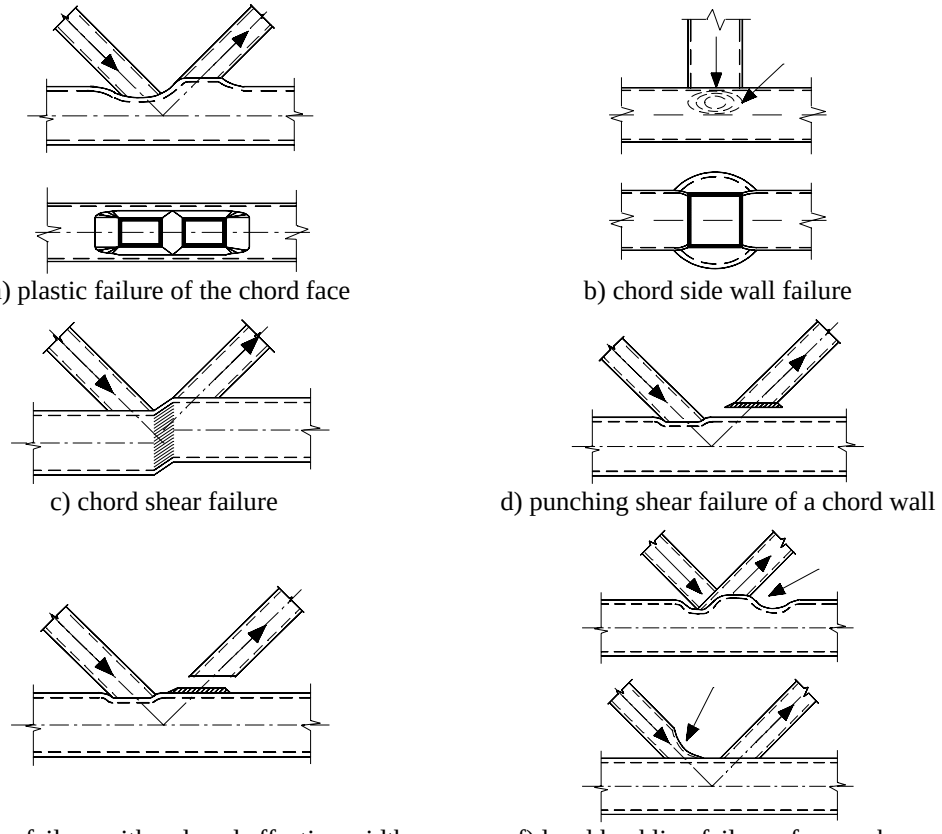

a) plastic failure of the chord face

b) chord side wall failure

c) chord shear failure

d) punching shear failure of a chord wall

e) brace failure with reduced effective width

f) local buckling failure of a member.

Figure 5: Eurocode3 failure modes [12].

For the “T” joint, the Eurocode provisions consider the failure of the RHS joint by mechanisms a), b), d), e) or f), and assume a range of validity of $\beta \geq 0{,}25$, $\mu_1 \leq 35$ and $\mu_0 \leq 35$.

For the structure considered in this work, the chords are 300×8 RHS sections and the braces 260×8 RHS sections. Therefore, the parameters of Figure 3 take the values of $\beta = 0{,}87$, $\mu_1 = 32{,}5$, $\mu_0 = 37{,}5$ and $\gamma = 18{,}8$. These values are slightly out of the Eurocode validity range, and consequently the corresponding results may be somewhat inconsequent.

The value of $\beta = 0{,}87$ is quite critical, since it may be easily observed from Figure 4 that a small variation of β in this zone corresponds to a very substantial variation of the plastic load from a bending mechanism. In addition, the problem in this particular structure is that the value of β is very close to the border between failure modes a) – for $\beta \leq 0{,}85$ - and d) - $\beta \geq 0{,}85$.

For the “KT” joint, the Eurocode 3 provisions consider these types of joints as a “K” joint, of a gap or overlap type, depending on the joint geometry. Since $\mu_0 = 37{,}5$, and the overlap ratio, λ_{ov} is 19 %, the current joint is again slightly out of the Eurocode rules range of validity that assume $\mu_0 \leq 35$ and $\lambda_{ov} \geq 25\%$.

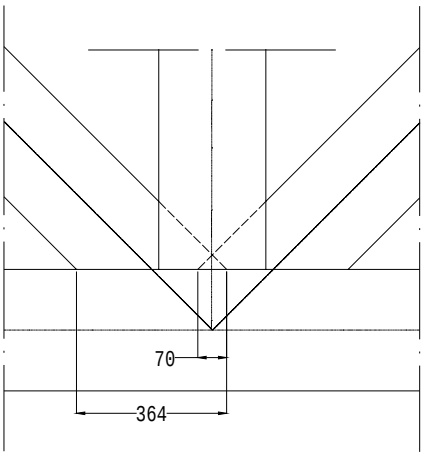

Figure 6: “KT” joint. Eurocode geometrical parameters

4 Finite Element Model

A finite element model for the studied geometries was developed using four-nodes thick shell elements, considering bending, shear and membrane deformations. The mesh was finer near the joint, where the stress concentration is higher, and the most regular as possible with well proportioned elements to avoid numerical problems.

Figure 7(a) shows the finite element model for a “T” joint. It is composed of 1320 nodes and 1288 elements. Figure 7(b) shows the equivalent model for the “KT” joint, with 1870 nodes and 1864 elements.

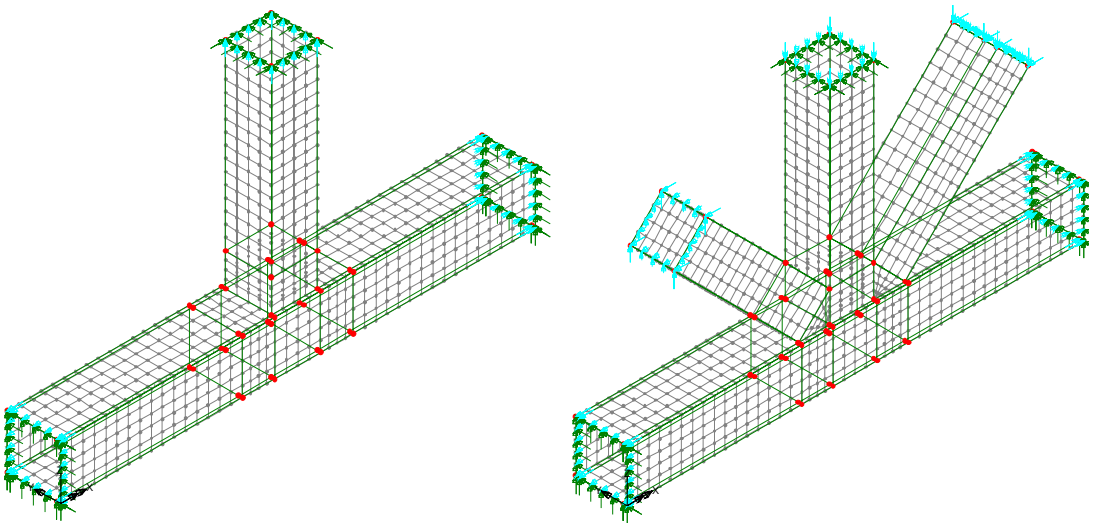

a) “T” Joint b) “KT” Joint

Figure 7: Numerical models to characterise “T” and “KT” joints.

The used material properties are: *Young* modulus E=210 *GPa*, *Poisson* coefficient υ=0.3. Two material types were considered: S275 and S355 steel grades with yield stresses of 275 and 355 *MPa* respectively.

For each model a linear analysis, a material nonlinear analysis, and a full material and geometric non linear analysis were performed. Therefore, it was possible to find the elastic stress distribution, and to detect first yielding at the connections. Besides that, the maximum numerical load could be compared to the plastic load calculated from the code [12]. The force-displacement curves for any node within the connection could be obtained as well, giving data for further considerations on the joint behaviour.

The full material and geometric non-linear analysis represents the full assessment of the safety of the joints, allowing the comparison between the EN 1993-1-8 [12] and the numerical results, and to evaluate the post-limit behaviour of the chord face.

5 Results

In this paragraph, for each considered joint type, the general behaviour is described, and the plastic load from the finite element analysis is presented. Furthermore, it is compared with the equivalent load calculated from the Eurocode [12] or other criteria.

5.1 “T” Joints

For the “T” joint, Figure 8 shows the results from the elastic analysis. For the load corresponding to the design combination of loads, the verification of the joint is presented in this picture through the deformed mesh (a) and the *von Mises* stresses (b). For this load factor of 1.5, corresponding to the factored design load, maximum stress is about 220 *MPa*, clearly below the plastic limit for both of the steel grades analyzed.

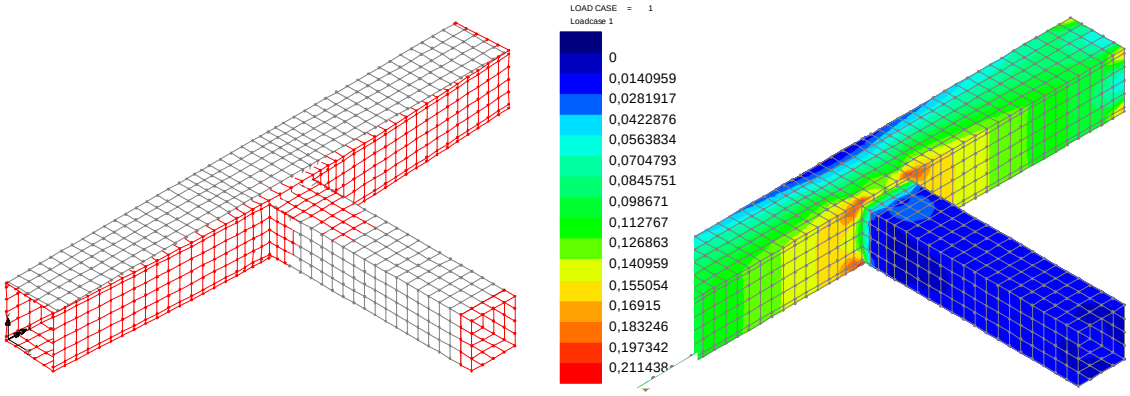

a) Deformed mesh b) *von Mises* stresses under the design load (*GPa*)

Figure 8: “T” joint. Deformed mesh and *von Mises* stresses under the design load

The onset of plasticity for grade S275 steel is shown in Figure 9, where the load factor applied is plotted with the evolution of the maximum *von Mises* stress. It may be concluded that the onset of plasticity corresponds to a load factor of more than 2.0, clearly higher than the minimum safety factor required of 1.5 in the context of an elastic analysis.

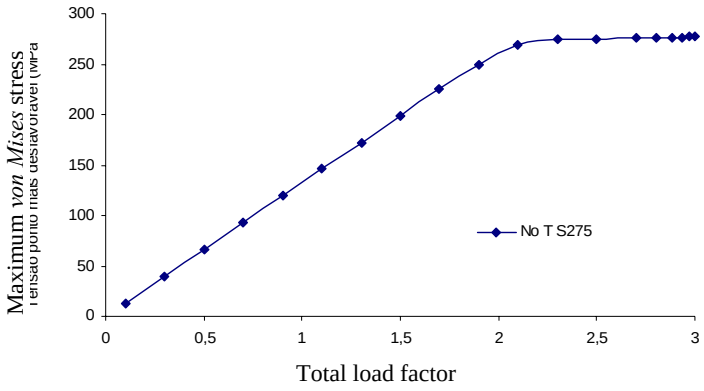

Figure 9: “T” joint. Load factor *versus* maximum *von Mises* stress

This analysis shows that the behaviour of the joint leads to more important stresses in the direction of the longitudinal axis of the chord member (around 180 *MPa* for the design load - Figure 10(a) than in the direction of the axis of the bracing member (around 80 *MPa* for the design load - Figure 10(b).

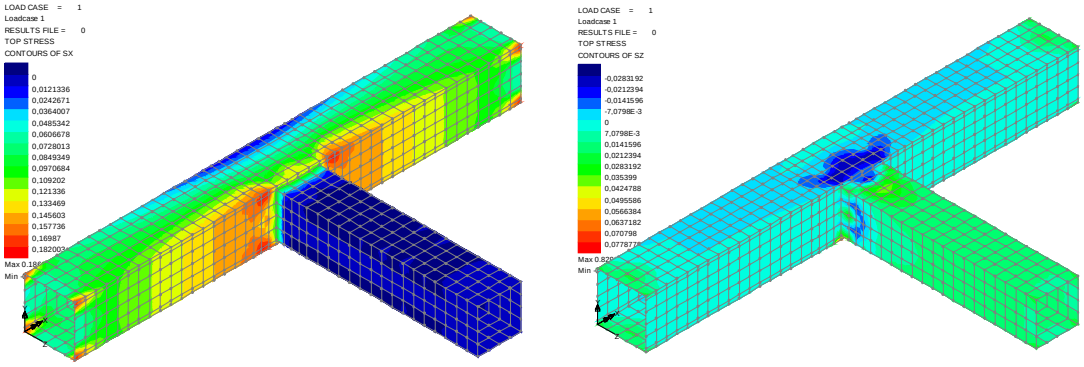

a) Stresses in direction X (chord axis) b) Stresses in direction Z (brace axis)

Figure 10: "T" joint. Stresses in directions X and Z

Plastic analysis of the joint shows that the collapse load corresponding to a full plastic mechanism accounting for bending and shear is, for the minimum yield stress (275 *MPa*), about 3 times the unfactored load imposed by the design combination of actions, as represented in Figure 11. The unfactored axial forces in the members (multiplying factor of 1.0) are shown as well. Again, this is clearly below the minimum required safety factor of 1.5 in the context of a plastic analysis.

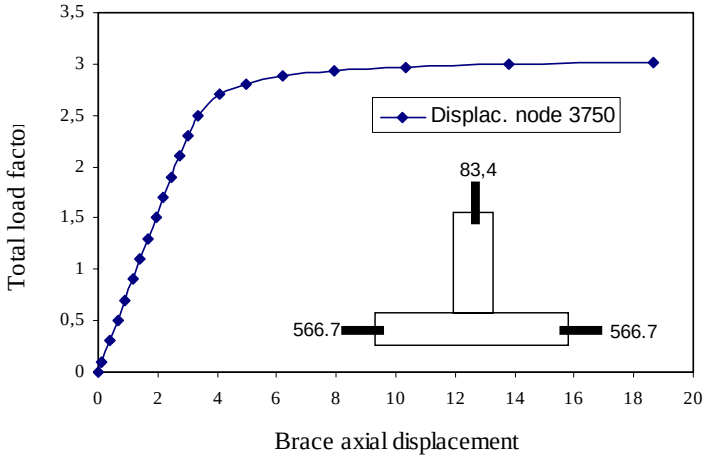

Figure 11: "T" joint. Load factor *versus* maximum displacement of the brace (geometrically linear analysis).

Figure 12 compares, for a representative node within the steel grade S275 "T" joint, the force *versus* displacement curve from a full nonlinear analysis to the Eurocode collapse load. This load corresponds to the weakest failure mode: a full

plastic mechanism at the chord face (full horizontal line in Figure 12).

In fact, Eurocode solution for this weakest mode (mode a – chord face failure) is 375 *kN* for S275 and 484 *kN* for S355 steel grades (accounting for the axial force in the chord member corresponding to the maximum load near the collapse).

The punching shear failure mode (mode d) corresponds to 836 *kN* and 1079 *kN* respectively for S275 and S355 steel grades.

It may be concluded that a quite substantial unsafe prediction of the bending plastic load is given by this code, most likely as the result of the particular value of $\beta = 0{,}87$. The Eurocode solution for $\beta = 0{,}85$, the upper limit of the validity range, is represented by the dotted line in the same figure.

Deformation criteria previously referred in this paper correspond to an out-of-plane displacement of the chord face of 9 *mm* (3% of the chord face width criterion) and 9.6 *mm* (1.2 times the chord face thickness criterion). The first criterion is also represented in Figure 12 by the vertical line, leading to a far more reasonable estimation of the ultimate limit state (approximately 250 *kN*) than the Eurocode3.

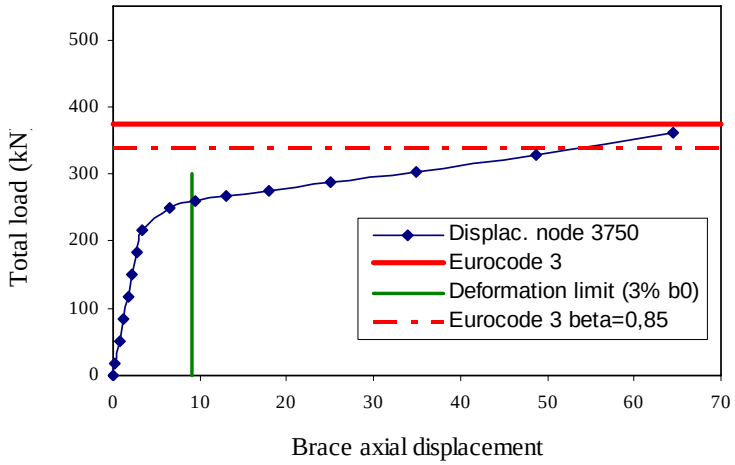

Figure 12: "T" joint S275 steel grade. Load factor *vs* maximum displacement of the brace (material and geometrically nonlinear analysis).

Similar results are shown in Figure 13 for grade S355 steel. The above adopted deformation criterion corresponds again to a more reasonable estimation of the ultimate limit state (approximately 325 *kN* as represented by the vertical line) than the Eurocode 3 solution based on bending mechanisms (full horizontal line).

Again, the dotted horizontal line corresponds to the validity limit of the Eurocode 3 for the chord face plastification ($\beta = 0{,}85$).

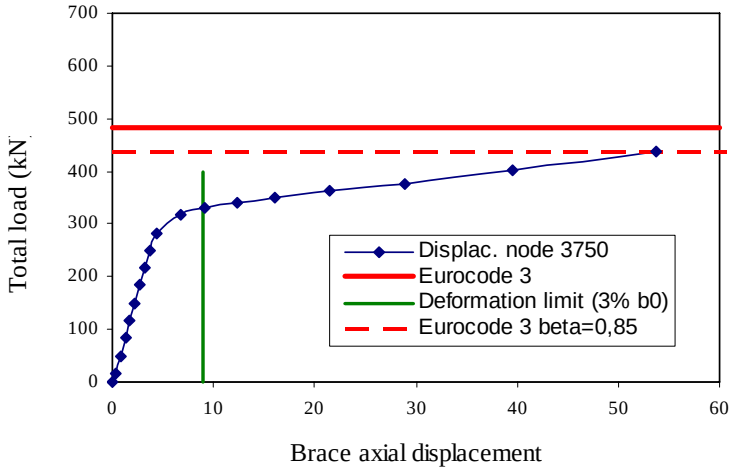

Figure 13: "T" joint S355 steel grade. Load factor *vs* maximum displacement of the brace (geometrically nonlinear analysis).

5.2 "KT" Joints

For the "KT" joint, Figure 14 shows the deformed mesh (a) and the *von Mises* stresses (b), corresponding to the onset of plasticity from a non-linear analysis for a steel S355 grade.

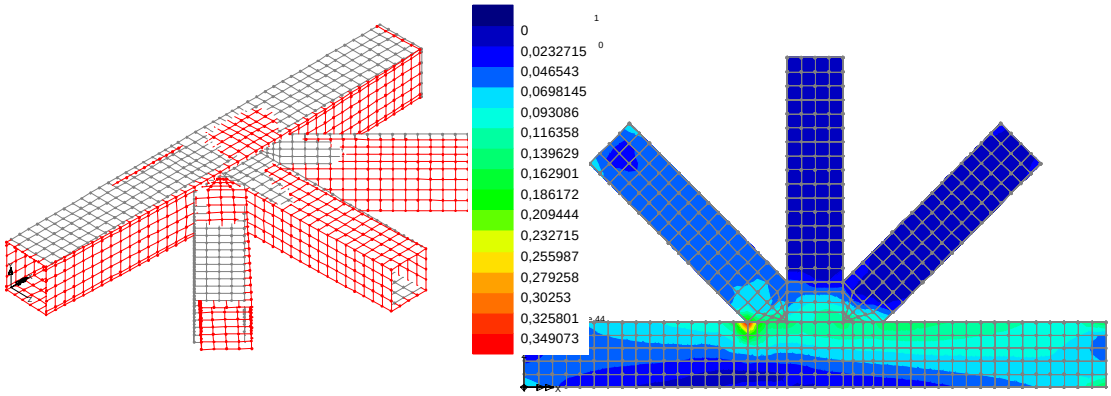

a) Deformed mesh b) von Mises stresses under design load (in *GPa*)

Figure 14: "KT" joint. Deformed mesh and *von Mises* stresses under unfactored load

When the load factor is 1.5, corresponding to the code recommended factored load for the design combination, maximum stress is about 180*MPa*, clearly below the plastic limit for both steel grades analyzed, as shown in Figure 15. In this figure, it can be spotted that the load factor corresponding to first yielding within the "KT" joint is of about 2.3.

Numerical analysis of the "KT" joint shows, similarly to the "T" joint, that stresses in the direction of the longitudinal axis of the chord member (Figure 16a)

are much higher than the stresses in the direction of the axis of the middle bracing member (Figure 16b).

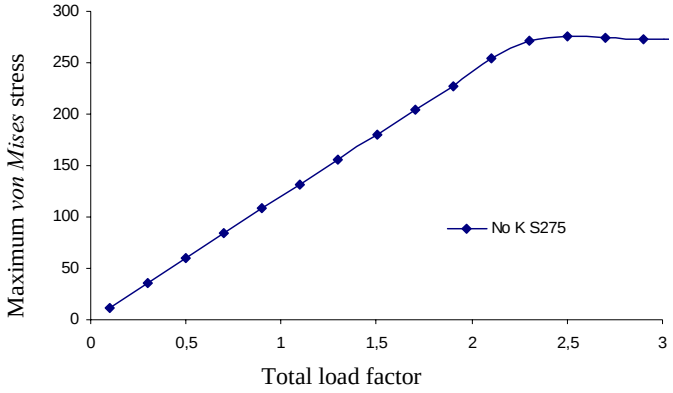

Figure 15: "KT" joint. Load factor *versus* maximum *von Mises* stress (S275 steel grade)

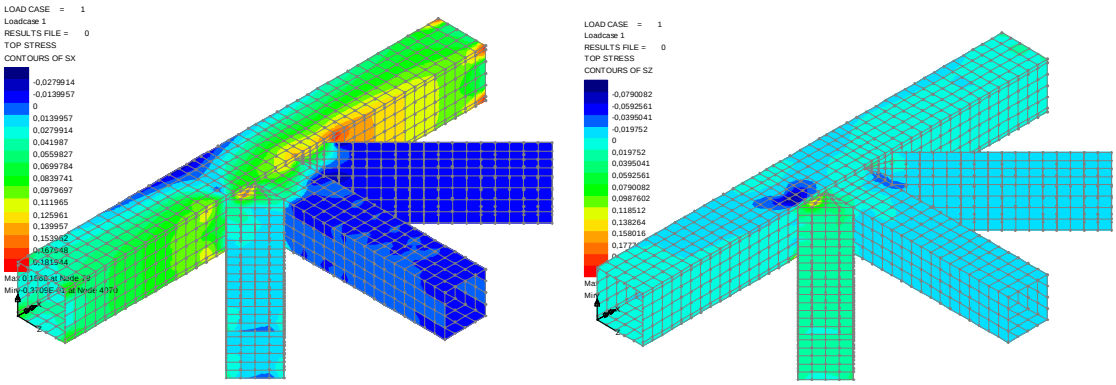

a) Stresses in direction X (chord axis) b) Stresses in direction Z (middle brace axis)

Figure 16: "KT" joint. Stresses in directions X and Z

Finite element plastic analysis of the joint without consideration of geometric nonlinearity presented in Figure 17 shows that the collapse load corresponding to a full plastic mechanism is 3.1 times the unfactored load of the relevant combination of actions for the design (grade S275 steel).

This value is clearly above the minimum required safety factor of 1.5 in the context of a plastic analysis. Also are shown in this figure the axial forces in the members for a multiplying factor of 1.0 for the relevant load combination.

The corresponding force *versus* displacement curve for the same case and for the same analysis is shown in Figure 18 where the comparison is made to the Eurocode 3 failure load that results from a brace failure mechanism, represented by the full horizontal line. This force is the resultant axial force in the most loaded brace

member (770*kN*). The application of Eurocode is out of its validity range, since the overlap ratio, λ_{ov} is 19%, smaller than the minimum of 25%. The same exercise using the minimum Eurocode value of $\lambda_{ov} = 25\%$, leads to a maximum load of 910*kN*, represented by the horizontal dotted line. It is worth to note that the maximum load obtained from this numerical plastic analysis without geometric nonlinearity is 841*kN* (corresponding to the above referred maximum load factor of 3.1 for the resultant force in the left member of Figure 17).

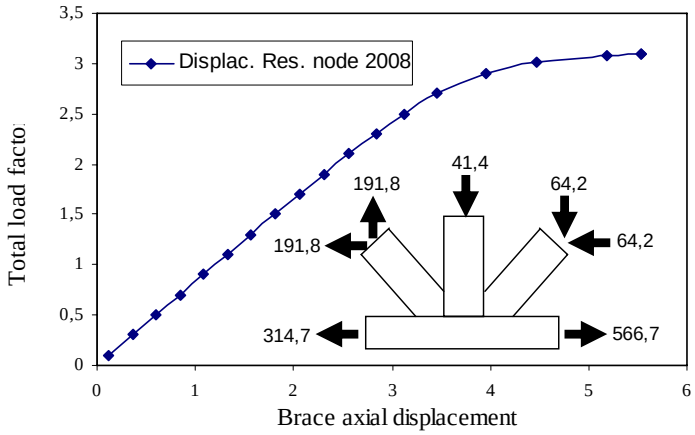

Figure 17: "KT" joint. Load factor *versus* maximum displacement of the brace (full plastic geometrically linear analysis and S275).

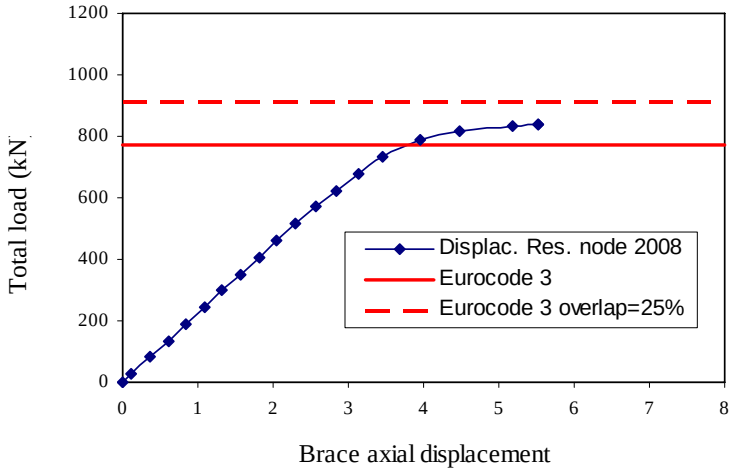

Figure 18: "KT" joint with S275 steel grade. Load factor *vs* maximum displacement of the brace (full plastic and geometrically nonlinear analysis)

Figure 19 shows, for the steel grade S355 "KT" joint, the force-displacement curve of a representative mesh node, resulting from a full nonlinear analysis. The Eurocode 3 failure load corresponding to a brace failure mechanism (994*kN*) is

represented by the full horizontal line. Again, application of Eurocode is out of its validity range ($\lambda_{ov} = 19\%$). The corresponding resistance value using $\lambda_{ov} = 25\%$ leads to a maximum load of 1175*kN*, represented by the horizontal dotted line.

Again, it is worth to note that the maximum load obtained from the finite element plastic analysis without geometric nonlinearity is 1085*kN* (corresponding to a maximum load factor of 4.0).

These numerical results are globally in line with the Eurocode 3 calculations, since the geometrical parameters affected by the lack of validity of the models are not so relevant for the brace failure than for the chord face failure in bending, shear, or punching shear.

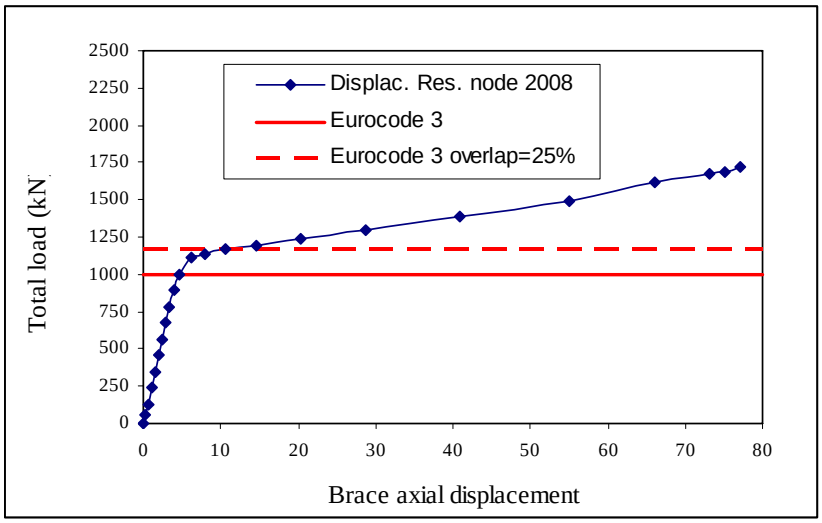

Figure 19: "KT" joint with S355 steel grade. Load factor *versus* maximum displacement of the brace (full plastic and geometrically nonlinear analysis).

6 Conclusions

A description of the application of the Eurocode 3 [12] models for the evaluation of a "T" and a "KT" joint was described. The geometries of these joints were slightly out of the code validity range.

It was found, for the "T" joint, that the joint fails by the chord face, and the parameter β plays a fundamental role on the joint resistance. The application of yield line bending mechanisms to relative large values of this parameter may lead to quite unsafe results. On the other hand, deformation limits criteria have shown to be adequate for the studied geometry.

The "KT" joint ruling failure mode is the brace failure, as predicted by the Eurocode. A reasonable agreement was found between these code provisions and the numerical results.

References

[1] CEN, Eurocode 3, EN1993-1-1: Design Steel Structures, May 2003, CEN, European Committee for Standardization, Brussels, 2003.

[2] Cao, J.J., Packer, J.A., Young, G.J., Yield line analysis of RHS connections with axial loads, *J. Constructional Steel Research, 1998 vol. 48, nº 1*, pp 1-25.

[3] Packer, J.A., Moment Connections between Rectangular Hollow Sections, *J.Constructional Steel Research 25,* 1993, pp 63-81.

[4] Packer, J.A., Wardenier, J., Kurobane, Y., Dutta, D., Yeomans, N., Assemblages de sections creuses rectangulaires sous chargement statique predominant. Série CIDECT "Construire avec des profiles creux", Verlag TUV Rheinland, Koln, 1993.

[5] Kosteski, N., Packer, J.A., Puthli, R.S., A finite element method based yield load determination procedure for hollow structural section connections, *J. Constructional Steel Research, vol. 59, nº 4*, pp. 427-559 (April 2003).

[6] Davies, G., Packer, J.A., Predicting the strenght of branch plate – RHS connections for punching shear, Canadian Journal of Civil Engineering, 9, nº 3, 1982, pp 458-467.

[7] Gomes, F.C.T., Etat Limite Ultime de la Résistance de L'âme d'une Colonne dans un Assemblage Semi-Rigide d'axe Faible, Rapport Interne nº 203, MSM - Université de Liège, 1990

[8] Korol, R., Mirza, F., Finite Element Analysis of RHS T-Joints, *Journal of the Structural Division, ASCE*, vol.108, No. ST9, Sep.1982, pp 2081-2098.

[9] Lu, L.H., de Winkel, G.D., Yu, Y., Wardenier, J., Deformation limit for the ultimate strength of hollow section joints, *6th International Symposium on Tubular Structures,* Melbourne, Australia, 1994, pp 341-347.

[10] Zhao, X, Hancock, G., T-Joints in Rectangular Hollow Sections Subject to Combined Actions, *Journal of the Structural Division, ASCE, vol.117, No. 8*, Aug.1991, pp2258-2277.

[11] Neves, L.F.C., Monotonic and Cyclic Behaviour of Minor-axis and Hollow Section Joints in Steel and Composite Structures, Doctoral Thesis, University of Coimbra, 2004.

[12] CEN, Eurocode 3, EN1993-1-8: Design of Joints, May 2003, CEN, European Committee for Standardization, Brussels, 2003.